



A NEW HIGH-FIDELITY TRANSIENT AEROTHERMAL MODEL FOR REAL-TIME SIMULATIONS OF THE T700 HELICOPTER TURBOHAFT ENGINE

Oğuz UZOL

Orta Doğu Teknik Üniversitesi Mühendislik Fakültesi Havacılık ve Uzay Mühendisliği Bölümü
06531 ODTÜ, Ankara, uzol@metu.edu.tr

(Geliş Tarihi: 05. 02. 2010, Kabul Tarihi: 14. 04. 2010)

Abstract: This paper presents a new transient aero-thermal model of the T700 helicopter turboshaft engine that is developed in order to simulate the critical transients that it may suffer during various operational conditions. The algorithm is composed of a set of differential equations and a set of non-linear algebraic equations representing each engine component. The compressor map is represented through a multi-layer neural network. The compressor bleed for turbine cooling and seal pressurization as well as the mixing of the turbine coolant flow with mainstream are also modelled. Mass flow and power imbalances during engine transients are modelled using the inter-component volumes method and the unsteady torque equation, respectively. Gas properties are calculated at each engine station using empirical relations that are functions of the local temperature. Open and closed-loop simulations are performed and the results are checked with previously published simulation data. Comparisons show good agreement both for steady state levels and transient responses. The model working in a closed-loop configuration together with a controller showed good potential in terms of simulating the variations of various engine related parameters during transient loading-unloading operations. The real-time capability of the model is also demonstrated such that the computational time taken by a single time step is about 2/3 of the time step of the physical simulation.

Keywords: Aerothermal model, Helicopter turboshaft engine, Real-time turboshaft model.

T700 HELİKOPTER TURBOŞAFT MOTORU GERÇEK-ZAMANLI SİMÜLASYONLARI İÇİN YENİ BİR YÜKSEK SADAKAT SEVİYELİ ZAMAN-BAĞIL AEROTHERMAL MODEL

Özet: Bu makale, T700 helikopter turboşaft motorunun çeşitli çalışma koşulları altında maruz kalabileceği kritik geçiş koşullarının simülasyonu amacı ile geliştirilen yeni bir zaman-bağıl aerothermal modeli sunmaktadır. Kullanılan algoritma motor bileşenlerini temsil eden diferansiyel ve cebirsel denklem setlerinden oluşmaktadır. Kompresör haritası çok katmanlı bir yapay sinir ağı kullanılarak temsil edilmiştir. Türbin soğutması ve sızdırmazlık sistemi basınçlandırması için kullanılan kompresör havası ile soğutma havasının ana akış ile karışması da modellenmektedir. Motor geçiş koşulları değişimi sırasındaki debi ve güç dengesizlikleri, sırası ile, bileşenler-arası hacim ve zamana-bağımlı tork denklemleri kullanılarak modellenmiştir. Her motor istasyonundaki gaz özellikleri lokal sıcaklığın fonksiyonu olan ampirik denklemler kullanılarak belirlenmektedir. Açık ve kapalı devre simülasyonlar yapılmış ve daha önceki çalışmalarda yayınlanan veriler ile karşılaştırılmıştır. Hem kararlı hal durumunda hem de geçiş durumunda daha önceki veriler ile uyumluluk gözlemlenmiştir. Model ile beraber çalışan bir kontrolcü kullanılarak yapılan kapalı-devre simülasyonlar, çeşitli yükleme-boşaltma durumlarındaki motor parametrelerinin değişiminin başarılı bir şekilde simüle edilebileceğini göstermiştir. Modelin gerçek-zamanlı çalışabilme kabiliyeti de kontrol edilmiş ve hesaplama için harcanan bir zaman adımının fiziksel simülasyon zaman adımının 2/3'ü olduğu görülmüştür.

Anahtar Kelimeler: Aerothermal model, Helikopter turboşaft motoru, Gerçek-zamanlı turboşaft modeli.

NOMENCLATURE

| | | | |
|-----------|--|------------|---|
| C_p | Specific heat at constant pressure [J/kgK] | M_{cc} | Air mass inside the combustor [kg] |
| g | air mass flow rate [kg/s] | N_1 | Gas generator rotational speed (Compressor-HPT) [rev/min] |
| g_b | fuel mass flow rate [kg/s] | N_2 | Power turbine rotational speed [rev/min] |
| h | total enthalpy [J/kg] | P_{atm} | Atmospheric pressure [Pa] |
| HPT | High Pressure Turbine | P_c | Compressor power [Watts] |
| J_{HPT} | HPT moment of inertia [Nms ²] | P_f | Power loss due to mechanical friction [Watts] |
| J_{PT} | PT moment of inertia [Nms ²] | P_{HPT} | HPT power [Watts] |
| LHV | Lower Heating Value of the fuel | P_{LOAD} | Load applied on the power turbine [Watts] |
| | | P_{PT} | Power turbine power [Watts] |

| | |
|------------|--|
| P_t | Total pressure [Pa] |
| PT | Power Turbine |
| R | Gas constant [J/kgK] |
| T_{atm} | Atmospheric temperature [K] |
| T_t | Total temperature [K] |
| V_p | Inter-component volume [m ³] |
| y_{loss} | Combustor pressure loss |

Greek symbols

| | |
|--------------|----------------------------------|
| β_c | Compressor pressure ratio |
| η_c | Compressor isentropic efficiency |
| η_b | Combustor efficiency |
| η_{HPT} | HPT isentropic efficiency |
| η_{PT} | PT isentropic efficiency |
| η_m | Mechanical efficiency |
| θ | T/T_{ref} |
| τ_{cc} | Combustor time constant [s] |

INTRODUCTION

Developing advanced and reliable gas turbine control algorithms requires high fidelity engine dynamic models. The transient dynamic simulations of gas turbines under various operating conditions performed using these dynamic models are of critical importance in order to ensure that the engine operates within safety limits in off-design conditions. These models could also be used for increasing the fidelity of real-time flight simulators by integrating the engine simulation algorithms with the flight dynamics modeling and simulation codes.

Structuring an aero-thermal model of a gas turbine engine is the first step to simulate engine performance in a dynamic manner as explained in detail in Walsh and Fletcher (1998). In previous work, non-linear aero-thermal models are developed using mathematical models which are composed of a set of differential equations plus a set of non-linear algebraic equations (e.g. Lichtsinder and Levy, 2006; Camporeale et al., 2002, 2006; Ballin, 1988). In these studies, aero-thermal models for various types of gas turbine engines are used to simulate real-time engine performance in order to either implement a control system to the engine or to monitor engine parameters for diagnostics. Some other mathematical models have also been developed in order to construct the simulation algorithm. A simplified mathematical model of a twin shaft gas turbine suitable for use in dynamic studies of both electric power generation plants and variable speed mechanical drive applications has been presented by Bozzi et al. (2003). Al-Hamdan and Ebaid (2006) have developed a mathematical model for each component using physical laws or empirical data when available. Instantaneous-response and transient-flow component models have been adapted for the prediction of the transient response of gas turbine cycles by Korakianitis et al. (2005). The simple mathematical gas turbine dynamic model developed by Kocer (2008), which used the beta-lines technique of Kurzke (1996) for compressor map

modelling, was used for the simulation of Hot Gas Ingestion problems in helicopter turboshaft engines (Kocer et al., 2008).

In this study, an aero-thermal model of T700 turboshaft engine is developed in order to simulate the critical transients that it may suffer during various operational conditions. These engines are used both in UH-60 Black Hawk as well as AH-1W Super Cobra helicopters that are currently operational in the Turkish Army. The algorithm is composed of a set of differential equations and a set of non-linear algebraic equations representing each engine component. The compressor map is represented through a multi-layer neural network. The compressor bleed for turbine cooling and seal pressurization as well as the mixing of the turbine coolant flow with mainstream are also modelled. Mass flow and power imbalances during engine transients are modelled using the inter-component volumes method and the unsteady torque equation, respectively. Gas properties are calculated at each engine station using empirical relations that are functions of the local temperature. Open-loop simulations are performed and the results are compared with previously published simulation data. In addition, closed-loop transient simulations are also performed using a PI controller acting as the engine governor. Details of the methodology and the results of these simulations are presented in the following sections.

METHODOLOGY

The transient aero-thermal mathematical model of the turboshaft engine consists of governing equations representing the aero-thermodynamic processes in each engine component. Figure 1 shows the engine station numbering used in the mathematical model. The input parameters that are needed to start up the simulation are the atmospheric conditions, gas and fuel properties, aerothermodynamic engine design variables, design point efficiencies and engine geometry related parameters as listed in Table 1.

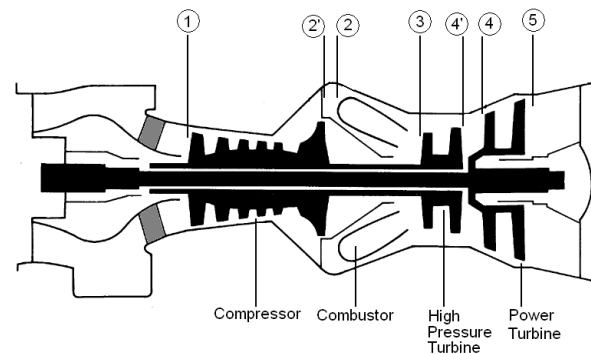


Figure 1. Turboshaft engine station numbering used in the transient aerothermal model.

Before starting the transient simulation, these input parameters are first used to obtain the steady state matched conditions inside the engine through a design

point cycle analysis. These matched conditions provide other initial thermodynamic states within the engine that are necessary to start up the simulation.

In order to capture the dynamic effects such as the mass flow and work imbalances during engine transients, the inter-component volumes method described in Fawke and Saravanamuttoo (1971) is used. Recent applications of this method to single and double-shaft engine configurations can be found in Gaudet (2007) and Camporeale et al. (2006). Two inter-component volumes are used to model and capture the mass accumulation inside the engine during transient operations: one between the compressor exit and the combustor inlet (between stations 2' and 2) and another one between the high-pressure turbine (HPT) exit and the power turbine (PT) inlet (between stations 4' and 4). The turbomachinery components are considered as

Table 1. Input parameters for the transient aerothermal turboshaft engine model.

| Properties | Physical Parameters | Symbols [Units] |
|---------------------------------------|----------------------------------|-------------------------------|
| Gas properties | Gas constant | R [J/kgK] |
| Fuel properties | Lower Heating Value | LHV [J/kg] |
| Atmospheric conditions | Temperature | T_{atm} [K] |
| | Pressure | P_{atm} [Pa] |
| Engine inlet conditions | Total Temperature | T_{t1} [K] |
| | Total Pressure | P_{t1} [K] |
| Engine design point parameters | Compressor Pressure Ratio | β_c |
| | Mass flow rate | g_1 [kg/s] |
| | Turbine inlet temperature | T_{t3} [K] |
| Engine design point efficiencies | Compressor isentropic efficiency | η_c |
| | Burner efficiency | η_b |
| | Burner pressure loss | y_{loss} |
| | HPT isentropic efficiency | η_{HPT} |
| | PT isentropic efficiency | η_{PT} |
| | Mechanical efficiency | η_m |
| Engine design point rotational speeds | HPT speed | N_1 [rev/min] |
| | PT speed | N_2 [rev/min] |
| Engine geometrical parameters | HPT inertia | J_{HPT} [Nms ²] |
| | PT inertia | J_{PT} [Nms ²] |
| | Inter-component volumes | V_p [m ³] |

volumeless elements and the combustor is considered as an energy accumulator only, similar to the study of Camporeale et al (2006). More details are given in the following sections.

Modeling of the Turbomachinery Components

The characteristics of the compressor during transient simulations are modelled using its performance map data given in Ballin (1988). The variation of the corrected mass flow with compressor pressure ratio at different corrected rotational speed values is represented through an artificial neural network. For this purpose, the Levenberg-Marquardt (LM) algorithm (Hagan and Menhaj, 1994) is used to train a two input single output system through a multi-layer perceptron network. This feed-forward network uses the corrected rotational speed and the pressure ratio values as inputs, i.e. two neurons in the input layer, and finds out necessary weighting coefficients to obtain the relevant output, i.e. the corrected mass flow (one neuron in the output layer). In this study, 9 and 18 neurons in the first and the second hidden layers are used, respectively, to accurately represent the characteristics. Hyperbolic tangent functions are used as network activation functions. Figure 2a presents the comparison of the data obtained from Ballin (1988) and its neural-network representation. As is evident the variations are correctly captured by the trained network. Examples of neural-network modelling of turbomachinery characteristics can be found in previous studies such as Ghorbanian and Gholamrezaei (2009) and Yu et al. (2007).

The variation of the temperature ratio of the compressor is also modelled using the data obtained from Ballin (1988), which presents the temperature ratio variation as a function of the pressure ratio. A third order polynomial is fit to this dataset, as shown in Figure 2b, and is used in the simulations.

The high pressure turbine (HPT) is assumed to be operating under choked flow conditions at all times. The power turbine characteristics are implemented through appropriate curve-fits to the variations of power turbine corrected mass flow rate and enthalpy drop data that are presented as functions of power turbine pressure ratio as given in Ballin (1988).

Gas Properties

The values for the specific heat at constant pressure (C_p) at different stations along the engine are calculated using the curve-fit polynomials given in Al-Hamdan and Ebaid (2006), which are functions of air or gas (i.e. combustion product) temperature at that specific location. Since the temperature values are initially unknown during a simulation, an iterative procedure is used to calculate the correct C_p value at each time step. These polynomial equations are included also here for completeness and they are obtained using the data given

in Chappel and Cockshutt (1974) as explained in Al-Hamdan and Ebaid (2006). The polynomial coefficients in equations 1 and 3 are presented in Table 2.

$$C_{p_a} = a + bT_a + cT_a^2 + dT_a^3 + eT_a^4 \quad (1)$$

$$C_{p_g} = C_{p_a} + \left(\frac{f}{1+f} \right) B_T \quad (2)$$

$$B_T = g + hT_g + iT_g^2 + jT_g^3 + kT_g^4 + lT_g^5 \quad (3)$$

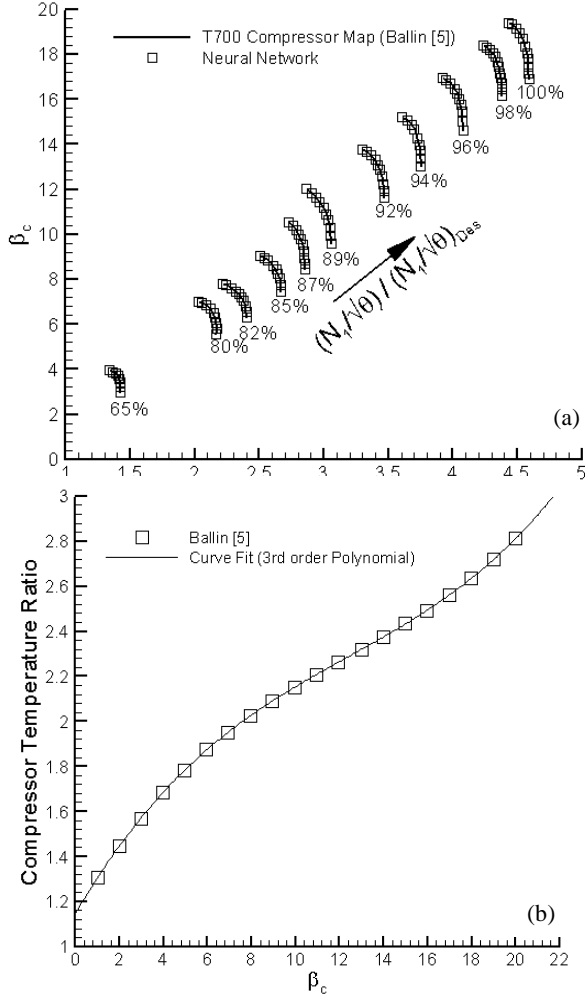


Figure 2. Representation of compressor characteristics in the transient aero-thermal model: (a) The compressor map as given in Ballin (1988) and its neural network representation, (b) compressor temperature ratio (Ballin, 1988) and the third-order polynomial curve-fit.

Unsteady Mass Balance

The unsteady mass balance within the engine that occurs during transient operations is modelled by introducing two separate adiabatic capacities in the engine similar to the studies by Camporeale et al. (2006) and Gaudet (2007). One of the capacities is placed right after the compressor (section 2'-2 in Figure 1) to take into account the mass flow rate imbalance between the HPT and the compressor, and the other capacity is placed between the HPT and the PT (section 4'-4 in Figure 1).

Table 2. Polynomial coefficients to be used in equations 1 to 3 for C_p calculation.

| Air (Equation 1) | Low Temperature Range (200 K -800 K) | High Temperature Range (800 K -2200 K) |
|----------------------|--------------------------------------|--|
| a | 1.0189×10^3 | 7.9865×10^2 |
| b | -0.13784 | 0.5339 |
| c | 1.9843×10^{-4} | -2.2882×10^{-4} |
| d | 4.2399×10^{-7} | 3.7421×10^{-8} |
| e | -3.7632×10^{-10} | 0.0 |
| Gas (Equations 2, 3) | Low Temperature Range (200 K -800 K) | High Temperature Range (800 K -2200 K) |
| g | -3.59494×10^2 | 1.0888×10^3 |
| h | 4.5164 | -0.1416 |
| i | 2.8116×10^{-3} | 1.916×10^{-3} |
| j | -2.1709×10^{-5} | -1.2401×10^{-6} |
| k | 2.8689×10^{-8} | 3.0669×10^{-10} |
| l | -1.2263×10^{-11} | -2.6117×10^{-14} |

The flow speed inside the plenum is assumed to be constant and the temperature and pressure inside the plenum are assumed to vary with a polytropic law with exponent m .

The unsteady mass balance is modelled through this adiabatic plenum by applying the conservation of mass and represented by the following equation as:

$$\frac{V_p}{mRT_{out}} \frac{dP_{out}}{dt} = g_{in} - g_{out} \quad (4)$$

where V_p is the volume of the plenum and the polytropic coefficient m is approximated by the specific heat ratio. The energy accumulation, pressure losses and momentum effects inside the plenum are all neglected. Therefore,

$$T_{out} = T_{in} \quad (5)$$

$$P_{out} = P_{in} \quad (6)$$

Combustor Dynamics

The combustor is modelled as an energy accumulator only neglecting the mass accumulation, which is already taken into consideration at the upstream plenum block. Inside the combustor, temperature and pressure values are assumed to be homogeneous and equal to the respective combustor outlet values. The combustor exit temperature is calculated using conservation of energy as:

$$\frac{dT_3}{dt} = \frac{[g_2 h_2 + g_b \eta_b LHV - g_3 h_3]}{g_3 C_{p3} \tau_{cc}} \quad (7)$$

where,

$$\tau_{cc} = \frac{M_{cc}}{kg_3} \quad (8)$$

Here, M_{cc} is the mass inside the combustor, LHV is the lower heating value of the fuel, τ_{cc} is the time constant, η_b is the combustor efficiency. The time constant, τ_{cc} is similar to an inertia term. For a bigger combustion chamber, M_{cc} term is larger resulting in a slower response to fuel addition in terms of combustor exit temperature increase. The total pressure at the combustor exit is calculated using the pressure loss value such as,

$$P_{t3} = y_{loss} P_{t2} \quad (9)$$

Shaft Dynamics

The shaft dynamics, i.e. the acceleration or the deceleration of the HPT or the PT spools due to the power imbalances during transients, are determined through the conservation of angular momentum as,

$$\frac{dN_1}{dt} = \frac{1}{J_{HPT} N_1} \left(P_{HPT} - P_c - P_{f_{HPT}} \right) \quad (10)$$

$$\frac{dN_2}{dt} = \frac{1}{J_{PT} N_2} \left(P_{PT} - P_{LOAD} - P_{f_{PT}} \right) \quad (11)$$

where, N_1 and N_2 are the HPT and the PT rotational speeds, respectively. P_{LOAD} is the load applied on the power turbine, P_f values are the amount of power loss due to mechanical friction and J values are the moments of inertia, which include the effects of the shaft and other connected devices.

Compressor Bleed and Coolant Mixing

The T700 engine has various bleed mechanisms that are used for different purposes such as pressurizing the seals inside the engine, pressurizing the power turbine balance piston and cooling the high pressure turbine blades and shrouds. The fractions of the bleed flow used for pressurizing the balance piston and for cooling purposes are presented as functions of the corrected compressor mass flow and the bleed fraction used for pressurizing the seals is given as a function of the gas generator speed in Ballin (1988). These bleed schedules are implemented to the current aero-thermal model through appropriate curve-fits to the available data.

The fraction of the bleed flow used for cooling the gas generator blades is re-introduced to the main gas path downstream of the high-pressure turbine. Related mass flow and enthalpy changes of the gas due to this process is calculated using,

$$g_{4r}' = g_4' + b_3 g_2' \quad (12)$$

$$h_{4r}' = \frac{g_4' h_4' + b_3 g_2' h_{4c}'}{g_4' + b_3 g_2'} \quad (13)$$

where b_3 is the bleed fraction and h_{4c}' is the enthalpy of the coolant fluid, which is assumed to be equal to the average of the enthalpies of the gas at the bleed and the coolant ejection points.

SIMULATION RESULTS

The transient aerothermal model described above is used for the open-loop and close-loop simulations of the T700 turboshaft engine. The simulation inputs and the design point specifications of the T700 engine are listed in Table 3. The values for some of these parameters are obtained from Ballin (1988) and others are estimated as indicated in Table 3.

Table 3. Input parameters and design point values for the transient aero-thermal simulation of the T700 engine

| Physical Parameter | Value |
|------------------------|---|
| R | 287 J/kgK |
| LHV | 42565836 J/kg ^(*) |
| T _{atm} | 288.15 K |
| P _{atm} | 101325 Pa |
| T _{t1} | Atmospheric |
| P _{t1} | |
| β _c | 17 ^(*) |
| g ₁ | 4.57 kg/s ^(*) |
| T _{t3} | 1500 K ^(**) |
| η _b | 0.985 ^(*) |
| y _{loss} | 0.988 ^(*) |
| η _m | 0.96 ^(**) |
| N ₁ | 44 700 rev/min ^(*) |
| N ₂ | 20 900 rev/min ^(*) |
| J _{HPT} | 0.06033 Nms ² ^(*) |
| J _{PT} | 0.08406 Nms ² ^(*) |
| V _{p1} | 0.004 m ³ ^(**) |
| V _{p2} | 0.004 m ³ ^(**) |
| (*) From Ballin (1988) | |
| (**) Estimated value | |

Open-Loop Simulations

The transient aerothermal model is first run in an open-loop mode where different schedules are applied directly to the fuel flow without a control system in order to observe variations in different engine parameters. These results are obtained by running the transient simulation within the required fuel flow range with a Δt of 0.001 seconds, and increasing the fuel flow in 0.0063 kg/s (50 lbm/min) steps every two seconds of the simulation (Figure 3). The steady state levels after the application of each step fuel change are used for the comparison of the steady state characteristics of the engine with available data obtained from Ballin (1988) as shown in Figures 3 through 5.

Figure 4 shows the steady state characteristics of the variation in the shaft power as the fuel flow is changed from 0.019 kg/s (150 lbm/min) to 0.107 kg/s (850 lbm/min). The results are compared with those of the real-time model by Ballin (1988) as well as the ones obtained by GE Status-81 and GE Unbalanced Torque Models as given also in (Ballin, 1988). As is evident, the steady state characteristics captured by the current model are consistent with the previously published ones in the literature.

Figure 5 shows the transient response of the current model to a step increase in the fuel flow rate level. The results are compared with those obtained with the real-time model by Ballin (1988) and the GE Status-81 model (Ballin, 1988). The fuel flow increases from a level of 0.0504 kg/s (400 lbm/h) to 0.09765 kg/s (775 lbm/h) 0.5 seconds after the start of the simulation. The variations in the turbine inlet temperature, gas generator rpm and the compressor exit static pressure are compared. Although the initial overshoot in the turbine inlet temperature level is higher both than the Ballin real-time model as well as the GE Status-81 model, the response quickly levels down and becomes consistent with the existing models. Both the gas generator rpm and the compressor exit static pressure levels are consistent with the published data.

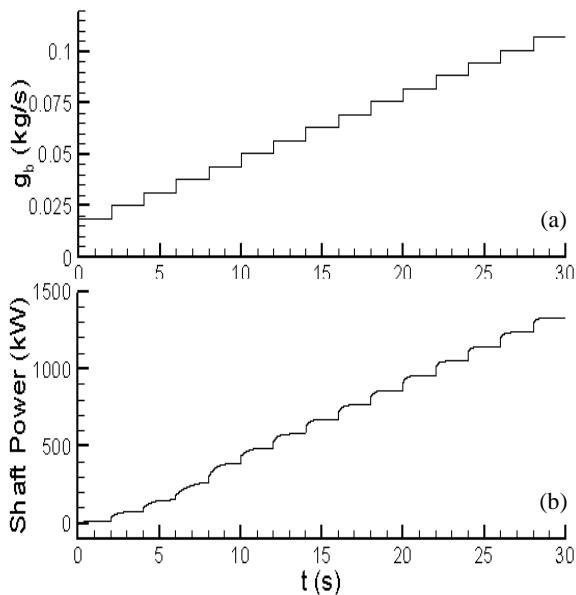


Figure 3. (a) Step-input fuel schedules applied for open-loop simulations and (b) corresponding variations in the engine shaft power.

Closed-Loop Simulations

The closed loop simulations are performed by applying step disturbances to the load applied on the power turbine. A PI controller controls the power turbine rotational speed, trying to keep it at a constant value by automatically changing the fuel mass flow rate. This mode of operation of the controller is typical both in

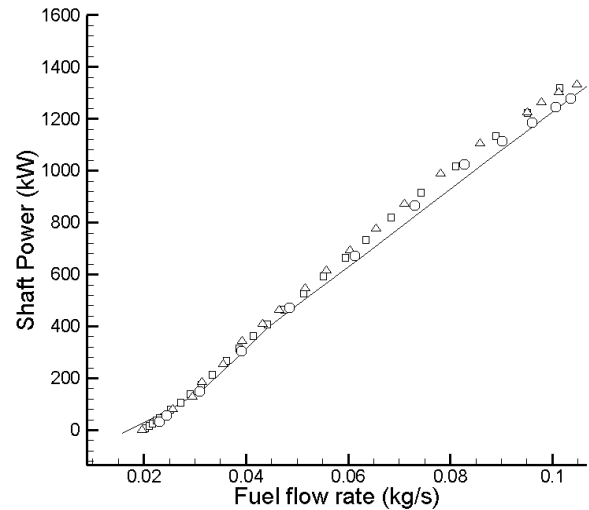


Figure 4. Comparison of the steady state power levels with previously published model data: Solid line: Current model; \square : Real-time model by Ballin (1988); Δ : GE Status-81 model (Ballin, 1988); \circ : GE Unbalanced Torque Model (Ballin, 1988).

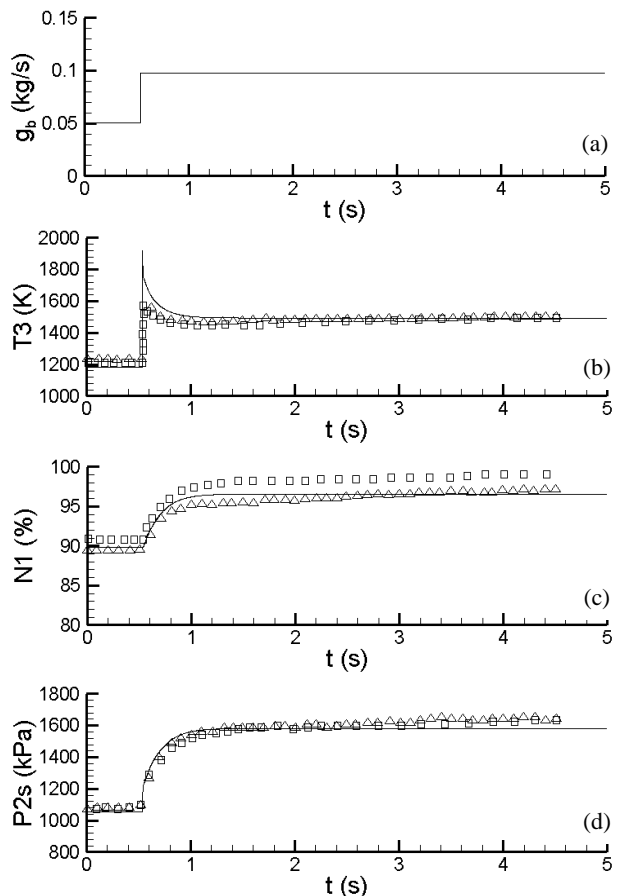


Figure 5. Transient response of the T700 engine model to a step increase in fuel flow rate. (a) fuel flow rate (b) turbine inlet temperature (c) gas generator rpm (d) compressor exit static pressure. Solid line: Current model; \square : Real-time model by Ballin (1988); Δ : GE Status-81 model (Ballin, 1988).

helicopter turboshaft engine applications as well as in electricity generating turbines where a constant output rpm is needed during engine transients.

Figure 6 shows the transient responses of several engine parameters to a 30% load drop on the power turbine at the 5th second of the simulation, which lasts 10 seconds and is followed by a 30% step-up loading on the power turbine bringing the power load to the starting level. All variables including the power load change are non-dimensionalized with their respective initial state values to be able to visualize the transient changes for all variables on the same plot.

As soon as the load drops down to 70% of the starting condition, the controller reduces the fuel flow rate to prevent an overspeed of the power turbine as shown in Figure 6a. The gas generator speed and the turbine inlet temperature levels (Figure 6b) change accordingly, consistent with the reduction in the fuel flow rate levels. At 15 seconds of the simulation the load on the power turbine is increased up 30% back to its original state, and the controller increases the fuel flow rate to prevent the power turbine from slowing down due to the load increase. As is evident from the figures, the power turbine speed remains constant during all these transients, with a slight overspeed and a slight deceleration at 5 s and 15 s of the simulation, respectively. All these variations are consistent with simulations performed for similar loading scenarios for different kinds of power generating turbines as reported in Camporeale et al. (2002, 2006).

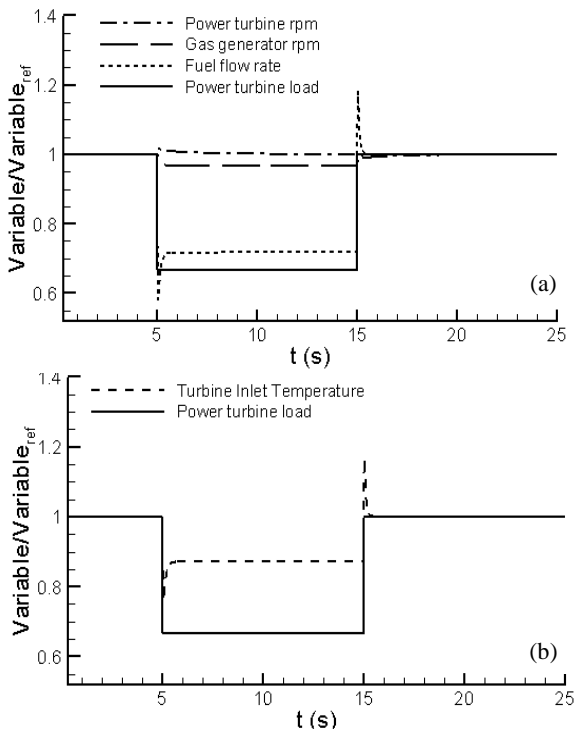


Figure 6. Closed-loop simulations of the transient response of the T700 engine model to step changes in power demand on the power turbine: (a) fuel flow, gas generator and power turbine speed variations, (b) turbine inlet temperature variation.

Figure 7 shows the variations in the compressor characteristics during the transient loading scenario

explained above. The reduction of the loading on the power turbine causes a reduction on the mass flow rate, rpm and the pressure ratio of the compressor. However, the compressor does not follow its steady state operating line and it goes through the transient following a different path as shown by the lower path line with triangular symbols in Figure 7. As is evident from the figure, the compressor passes close to its choke boundary during the first part of this transient where a load drop occurs on the power turbine. After the load is re-applied, the compressor returns to its starting point following a different path marked by the square symbols, which now takes it close to its stall boundary. These trends in the transient paths are also consistent with previously published simulations described by Camporeale et al. (2002, 2006) and provide useful information and predictions as to how close the engine (or the compressor) will get close to its operational boundaries during transient operations.

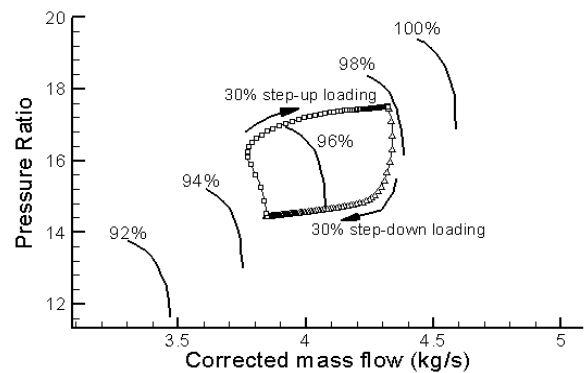


Figure 7. Compressor performance changes during the transient loading scenario described in Figure 6.

Real-Time Simulation Considerations

The executable simulation program that is produced from a FORTRAN 90 source code is tested also for its real-time capability. For this purpose the “cpu_time()” intrinsic subroutine is called before and after the simulation loop for the closed-loop test case described above. The simulation is performed for 25,000 time steps corresponding to 25 seconds of simulation with a time step size of 1 ms. The average computer time per time step is calculated by dividing the total elapsed time by the total number of time steps, and is found out to be 0.67 ms on a laptop computer with 1.7 GHz Pentium-M processor and 1 Gb of memory. Note that the computational work needed for a single time step does not change during the simulation. Therefore the computer simulations are running about 1.5 times faster than the simulated system, even on this relatively less powerful computer, resulting in the conclusion that the simulation code can be used in real-time applications.

CONCLUSIONS

A new transient high-fidelity aero-thermal model of the T700 helicopter turboshaft engine is presented. The

model includes neural-network representation of the compressor characteristics, inter-component volume modelling of mass accumulation during transients, modelling of the compressor bleed and coolant mixing ejected from the high pressure turbine and variable gas properties through the engine gas path. The new model is compared with previously published simulation data in the open literature and showed good agreement both for steady state levels and transient responses. The model working in a closed-loop configuration together with a controller showed good potential in terms of simulating the variations of various engine related parameters during transient loading-unloading operations. The real-time capability of the model is also demonstrated such that the computational time taken by a single time step is about 2/3 of the time step of the physical simulation. The new transient aerothermal model is proven to be as accurate as the existing models. It is also easier to use and less costly due to the application of neural network based turbomachinery component representations.

REFERENCES

- Al-Hamdan, Q. Z. and Ebaid, M. S. Y., Modelling and Simulation of a Gas Turbine Engine for Power Generation, *ASME Journal of Engineering for Gas Turbines and Power* 128, 302-311, 2006.
- Ballin, M. G., A High-Fidelity Real-Time Simulation of a Small Turboshift Engine, *NASA-TM-100991*, 1988.
- Bozzi, L., Crosa, G. and Trucco, A., Simplified Block Diagram of Twin Shaft Gas Turbines, *Proceedings of ASME Turbo Expo Power for Land, Sea and Air*, 2003.
- Camporeale, S. M., Fortunato, B. and Mastrovito, M., A Modular Code For Real-Time Dynamic Simulation of Gas Turbines in Simulink, *ASME Journal of Engineering for Gas Turbines and Power* 128, 506-517, 2006.
- Camporeale, S. M., Fortunato, B. and Mastrovito, M., A High Fidelity Real-Time Simulation Code of Gas Turbine Dynamics For Control Applications, *ASME paper GT-2002-30039*, 2002.
- Chappel, M. S. and Cockshutt, E. P., Gas Turbine Cycle Calculations: Thermodynamic Data Tables for Air and Combustion Products for Three Systems of Units, *NRC No: 14300, Ottawa, Canada, 1974.*
- Fawke, A. J. and Saravanamuttoo, H. I. H., Digital Computer Methods for Prediction of the Gas Turbine Dynamic Response, *SAE Paper 710550, SAE Mid-Year meeting, Montreal, Canada, 1971.*
- Gaudet, S. R., Development of a Dynamic Modeling and Control System Design Methodology for Gas Turbines, *Master of Applied Science Thesis, Department of Mechanical and Aerospace Engineering, Carleton University, Ottawa, Ontario, Canada, 2007.*
- Ghorbanian, K. and Gholamrezaei, M., An Artificial Neural Network Approach to Compressor Performance Prediction, *Applied Energy* 86, 1210-1221, 2009.
- Hagan, M. T. and Menhaj, M., Training feedforward networks with the Marquardt algorithm, *IEEE Transactions on Neural Networks* 5, 6, 989-993, 1994.
- Kocer, G., Aerothermodynamic Modeling and Simulation of Gas Turbines for Transient Operating Conditions, *MS Thesis, Department of Aerospace Engineering, Middle East Technical University, 2008.*
- Kocer, G., Uzol, O. and Yavrucuk, I., Simulation of the Transient Response of a Helicopter Turboshift Engine to Hot Gas Ingestion, *Proceedings of ASME Turbo Expo 2008: Power for Land, Sea and Air, GT2008-51164, June 9-13, Berlin, Germany, 2008.*
- Korakianitis, T., Hochstein, J. I. and Zou, D., Prediction of the Transient Thermodynamic Response of a Closed-Cycle Regenerative Gas Turbine, *ASME Journal of Engineering for Gas Turbines and Power*, 127, 57-64, 2005.
- Kurzke, J., How To Get Component Maps For Aircraft Gas Turbine Performance Calculations, *Proceedings of The International Gas Turbine and Aeroengine Congress and Exhibition*, 1996.
- Lichtsinder, M. and Levy, Y., Jet Engine Model For Control and Real-Time Simulations, *ASME Journal of Engineering for Gas Turbines and Power*, 128, 745-753, 2006.
- Walsh, P. P. and Fletcher, P., *Gas Turbine Performance*, Blackwell Science, Oxford, 1998.
- Yu, Y., Chen, L., Sun, F. and Wu, C., Neural-Network Based Analysis and Prediction of a Compressor's Characteristic Performance Map, *Applied Energy*, 84, 48-55, 2007.



Oguz UZOL received his BS and MS degrees in 1992 and 1995, respectively, from the Department of Aeronautical Engineering at The Middle East Technical University. He received his PhD degree from the Department of Aerospace Engineering at The Pennsylvania State University in 2000. He worked as a Post-Doctoral Fellow in the Department of Mechanical Engineering at The Johns Hopkins University from 2001 till 2005, and he joined the Department of Aerospace Engineering at The Middle East Technical University the same year. He is currently an Assistant Professor of Aerospace Engineering in the same department. His research interests include gas turbine simulation and modeling, experimental research in turbulence and aerodynamics.